

SUPPLEMENTARY INFORMATION

Biodistribution studies of ultrasmall silicon nanoparticles and carbon dots in experimental rats and tumor mice

Nadia Licciardello^{1,2,3#}, Sebastian Hunoldt^{1#}, Ralf Bergmann¹, Garima Singh¹, Constantin Mamat¹, Angélique Faramus^{2,3}, John L. Z. Ddungu^{2,3}, Simone Silvestrini⁴, Michele Maggini⁴, Luisa De Cola^{2,3*}, Holger Stephan^{1*}

¹Institute of Radiopharmaceutical Cancer Research, Helmholtz-Zentrum Dresden - Rossendorf, Bautzner Landstraße 400, Dresden, D-01328, Germany

²Laboratoire de Chimie et des Biomatériaux Supramoléculaires, Institut de Science et d'Ingénierie Supramoléculaires (ISIS), 8 allée Gaspard Monge, Strasbourg, 67000, France

³Institut fuer Nanotechnologie (INT), Karlsruher Institut fuer Technologie (KIT) Campus North, Hermann-von-Helmholtz-Platz 1, Eggenstein-Leopoldshafen, 76344, Germany

⁴Department of Chemical Sciences, University of Padova, Via Marzolo 1, 35131 Padova, Italy

These authors contributed equally.

Corresponding authors:

Dr. Holger Stephan, Helmholtz-Zentrum Dresden - Rossendorf, Institute of Radiopharmaceutical Cancer Research, Bautzner Landstrasse 400, 01328 Dresden, Germany, Phone: +49 3512603091, Fax: +49 3512603232, E-Mail: h.stephan@hzdr.de

Prof. Luisa De Cola; Laboratoire de Chimie et des Biomatériaux Supramoléculaires, Institut de Science et d'Ingénierie Supramoléculaires (ISIS), 8 allée Gaspard Monge, Strasbourg, 67000, France, Phone: +33 368855220; Fax: +33 368855242, E-Mail: decola@unistra.fr

Table of contents:

- Figure S1** Emission spectra at various excitation wavelengths of Si NPs-micro (**A**), Si NPs-hydro (**B**) in water and CQDs (**C**) in ethanol.
- Figure S2** ATR-FTIR spectra of Si NPs-micro (**A**), Si NPs-hydro (**B**) and CQDs (**C**).
- Figure S3** Zeta potential of nanoparticle-batches in dependence of increasing amount of NOTA-Bn-SCN; values given as mean of 3 different measurements; standard-deviation in between maximum peak half width.
- Figure S4** ^1H NMR spectrum of Si NPs-hydro (red line) and trisodium citrate (small spectrum, green line) measured in D_2O (solvent signal: $\delta = 4.79$ ppm).
- Figure S5** ^{13}C NMR spectrum of Si NPs-hydro measured in D_2O .
- Figure S6** ^1H - ^{13}C HSQC spectrum of Si NPs-hydro measured in D_2O .
- Figure S7** Superimposition of ATR-FTIR spectra of trisodium citrate (black line) and of Si NPs-hydro (red line).
- Figure S8** Radio-thin layer chromatograms (iTLC-SA plates) of $[^{64}\text{Cu}]\text{Cu-EDTA}$, $[^{64}\text{Cu}]\text{Cu-NOTA-Si NP-hydro}$, $[^{64}\text{Cu}]\text{Cu-NOTA-Si NP-micro}$ and $[^{64}\text{Cu}]\text{Cu-NOTA-CQDs}$ developed in 0.9% NaCl in H_2O .
- Figure S9** Orthogonal sections and maximum intensity projections of PET studies as separate PET and combined PET/CT images of $[^{64}\text{Cu}]\text{Cu-NOTA-CQDs}$ at 60 min p.i. in two A431 tumor-bearing mice after single intravenous injection.
- Figure S10** *Ex vivo* fluorescence images of whole body freeze sections of NMRI nu/nu mice at different times after single intravenous injection of Kodak-XS-670-labeled Si NPs-micro.
- Figure S11** Tumor to tissue time curves derived from kinetic PET studies of $[^{64}\text{Cu}]\text{Cu-NOTA-Si NPs-hydro}$, $[^{64}\text{Cu}]\text{Cu-NOTA-Si NPs-micro}$ and $[^{64}\text{Cu}]\text{Cu-NOTA-CQDs}$ in A431 tumor-bearing mice after single intravenous injection.
- Table S1** Amount of $[^{64}\text{Cu}]\text{Cu-NOTA-Si NPs-hydro}$, $[^{64}\text{Cu}]\text{Cu-NOTA-Si NPs-micro}$, and $[^{64}\text{Cu}]\text{Cu-NOTA-CQDs}$ in selected organs, and excretion in rats at different times after single intravenous application.
- Table S2** Concentration of $[^{64}\text{Cu}]\text{Cu-NOTA-Si NPs-hydro}$, $[^{64}\text{Cu}]\text{Cu-NOTA-Si NPs-micro}$ and $[^{64}\text{Cu}]\text{Cu-NOTA-CQDs}$ in selected organs, tissues, and excretion in rats at different times after single intravenous application.
- Table S3** Best fit values according to the one-phase decay model of the $[^{64}\text{Cu}]\text{Cu-NOTA-Si NPs-hydro}$, $[^{64}\text{Cu}]\text{Cu-NOTA-Si NPs-micro}$ and $[^{64}\text{Cu}]\text{Cu-NOTA-CQDs}$ clearance from the blood.
- Table S4** Best fit values according to the one-phase association model of the $[^{64}\text{Cu}]\text{Cu-NOTA-Si NPs-hydro}$, $[^{64}\text{Cu}]\text{Cu-NOTA-Si NPs-micro}$ and $[^{64}\text{Cu}]\text{Cu-NOTA-CQDs}$ accumulation in the urine.

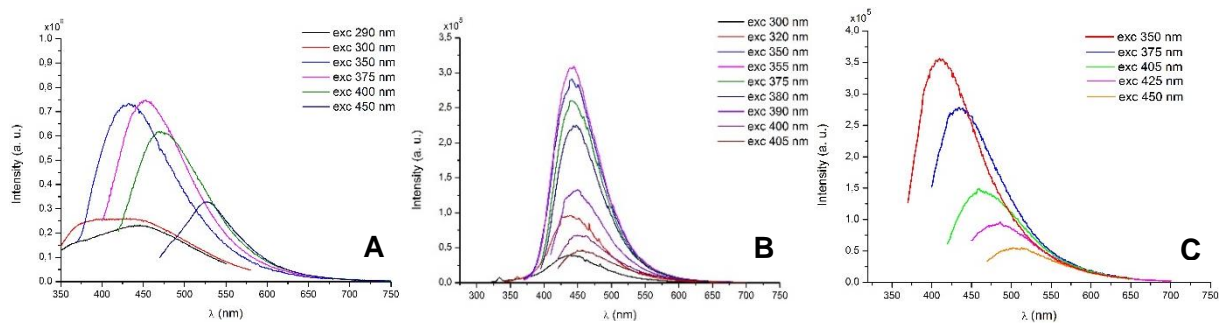


Figure S1 Emission spectra at various excitation wavelengths of Si NPs-micro (A), Si NPs-hydro (B) in water and CQDs (C) in ethanol.

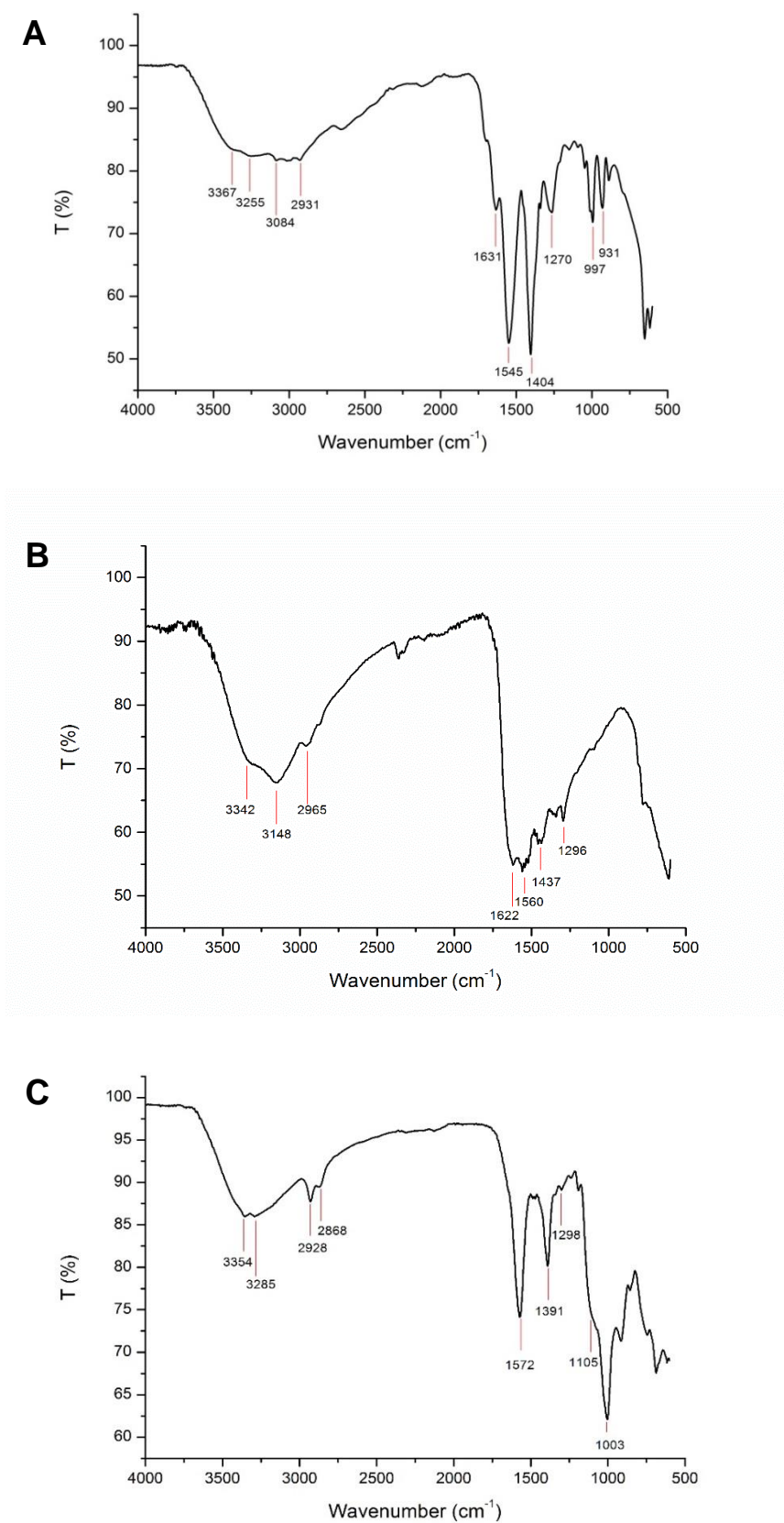


Figure S2 ATR-FTIR spectra of Si NPs-micro (**A**), Si NPs-hydro (**B**) and CQDs (**C**).

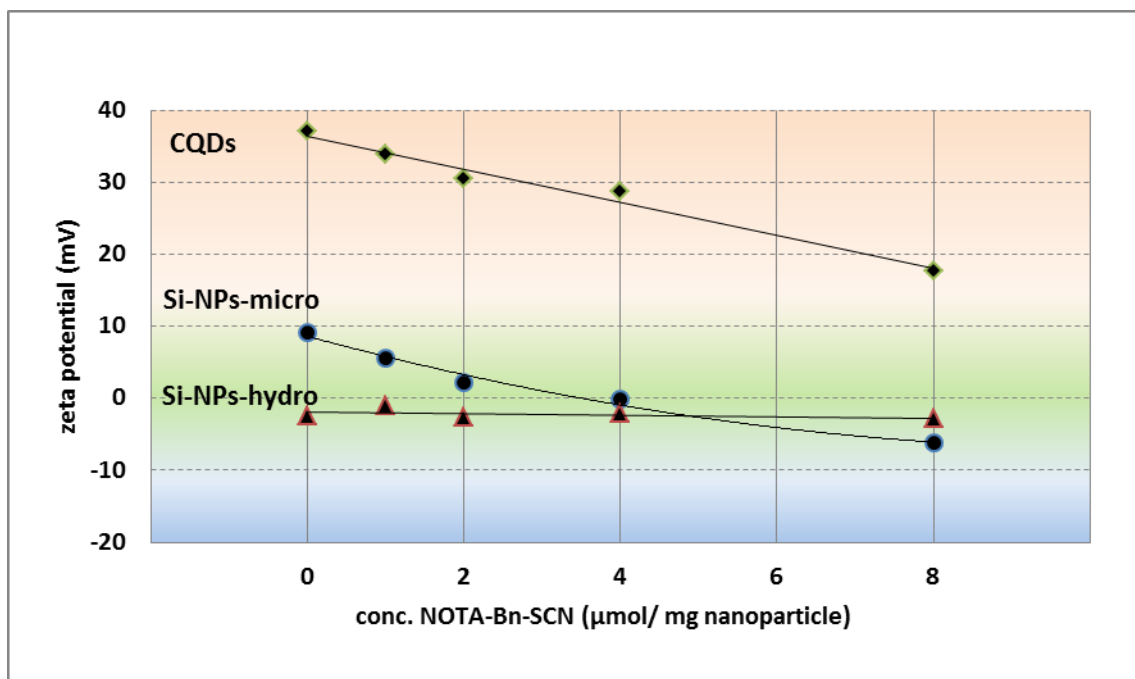


Figure S3 Zeta potential of nanoparticle-batches in dependence of increasing amount of NOTA-Bn-SCN; values given as mean of 3 different measurements; standard-deviation in between maximum peak half width.

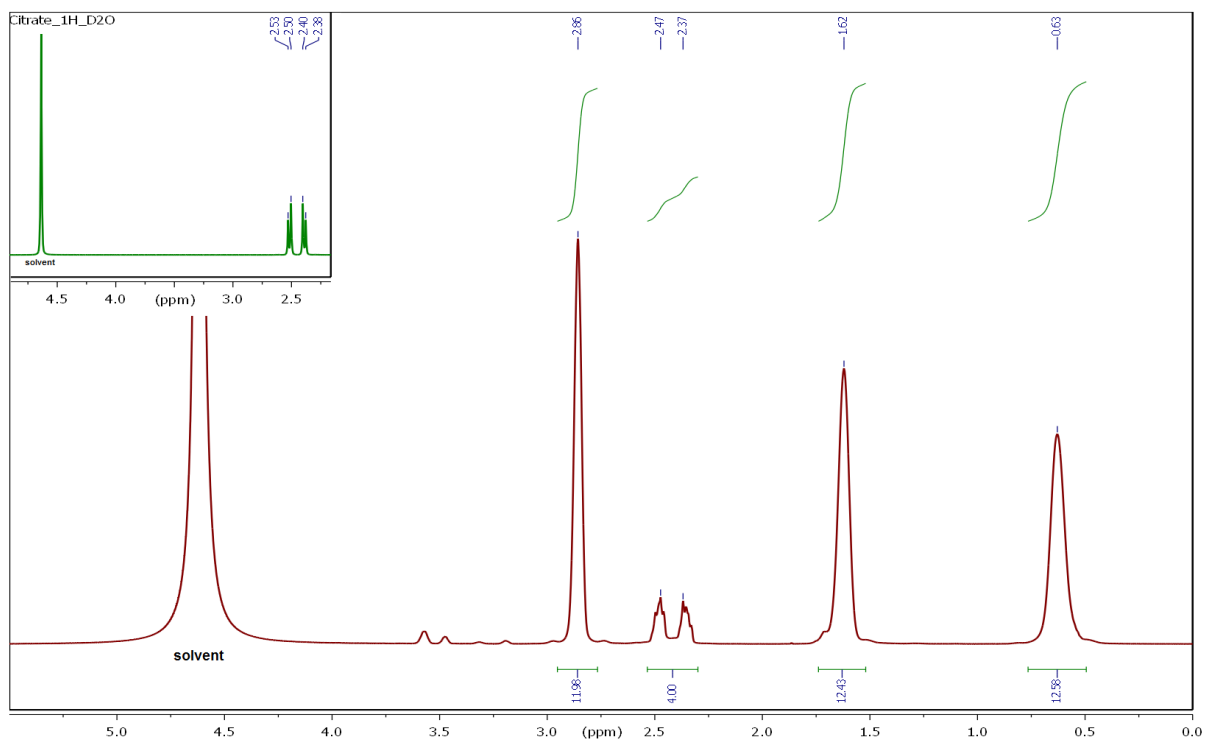


Figure S4 ^1H NMR spectrum of Si NPs-hydro (red line) and trisodium citrate (inset: green line) measured in D_2O (solvent signal: $\delta = 4.79$ ppm).

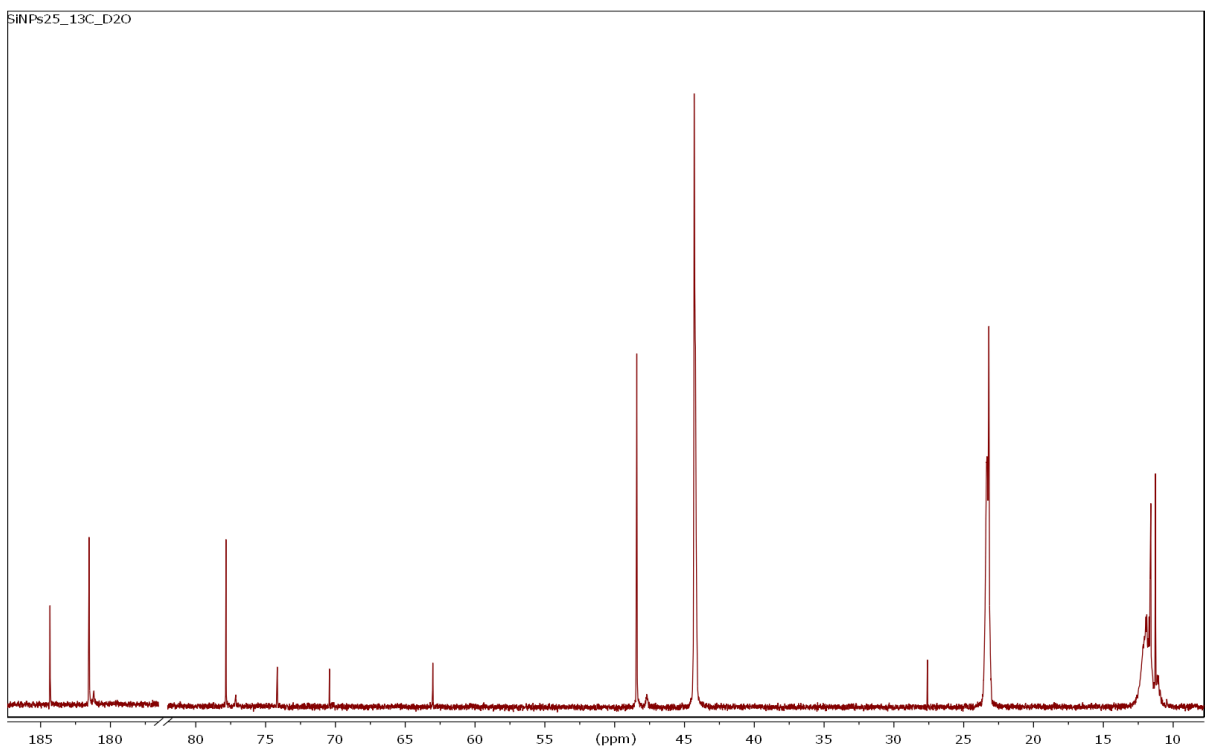


Figure S5 ^{13}C NMR spectrum of Si NPs-hydro measured in D_2O .

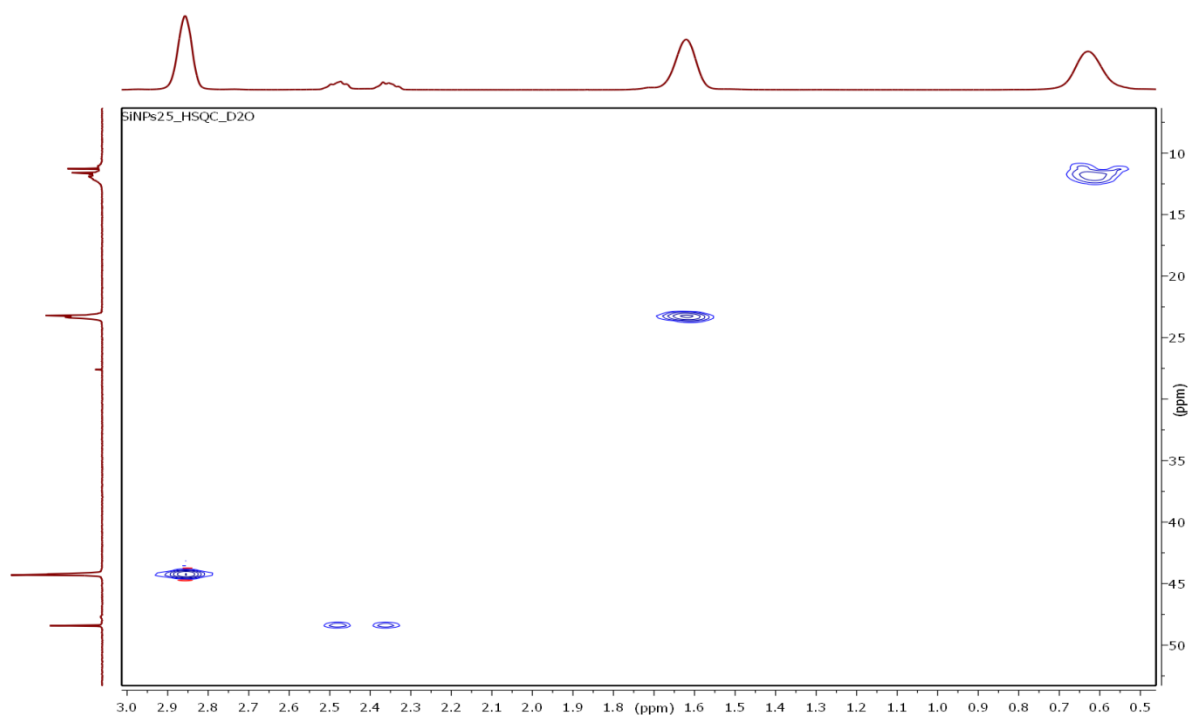


Figure S6 ^1H - ^{13}C HSQC spectrum of Si NPs-hydro measured in D_2O .

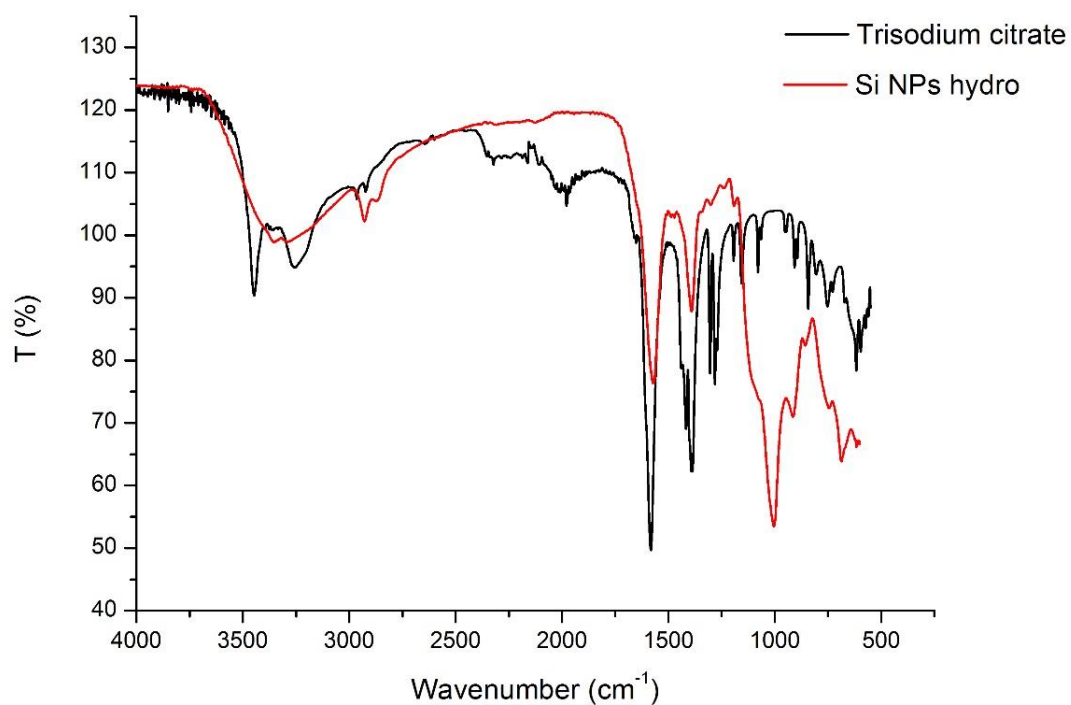


Figure S7 Superimposition of ATR-FTIR spectra of trisodium citrate (black line) and of Si NPs-hydro (red line).

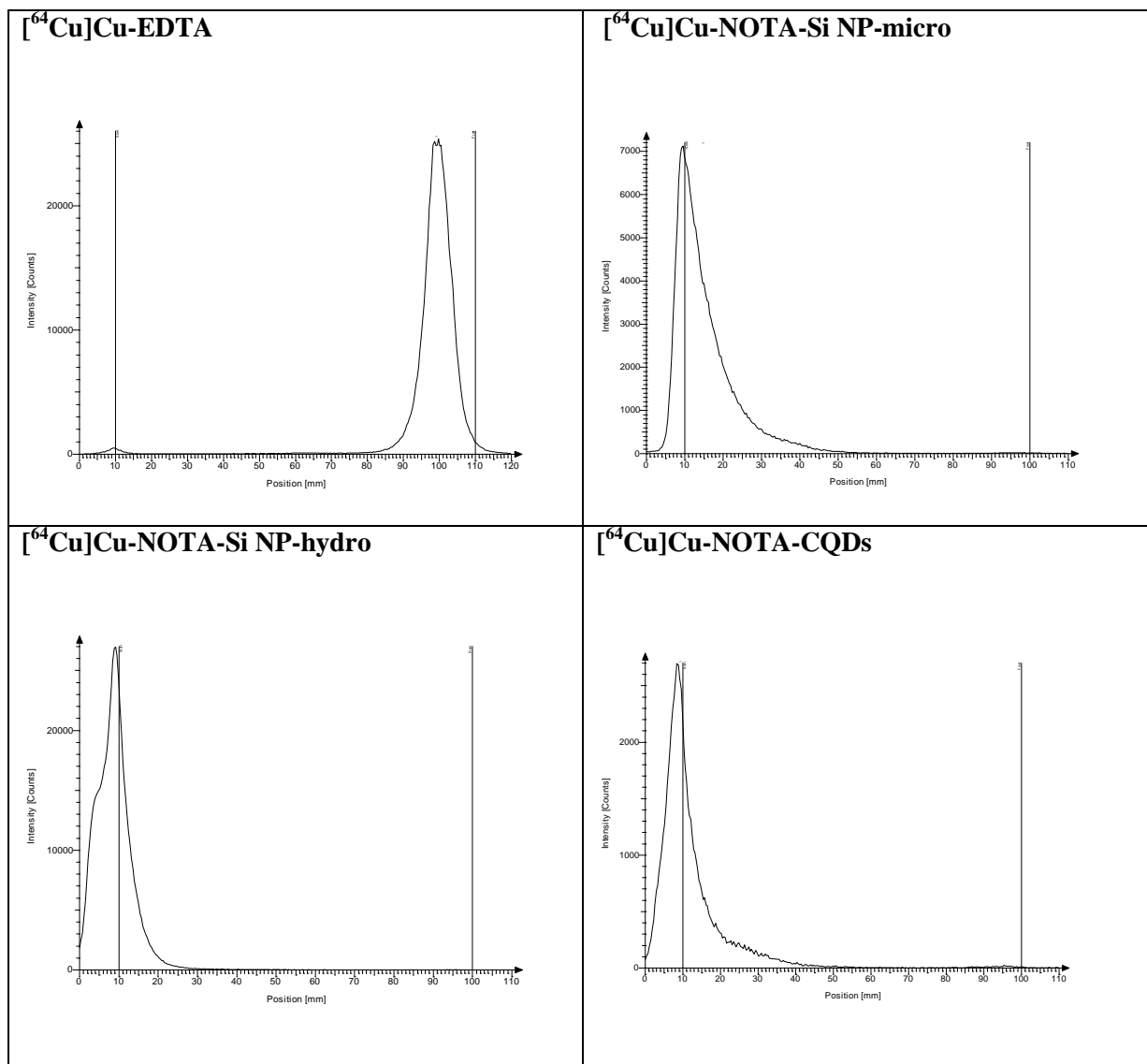


Figure S8 Radio-thin layer chromatograms (iTLC-SA plates) of ^{64}Cu Cu-EDTA, ^{64}Cu Cu-NOTA-Si NP-hydro, ^{64}Cu Cu-NOTA-Si NP-micro and ^{64}Cu Cu-NOTA-CQDs developed in 0.9% NaCl in H_2O . ^{64}Cu Cu-EDTA moves (^{64}Cu Cu-EDTA: $R_f = 0.9$); ^{64}Cu -labeled NPs stay at the origin (start).

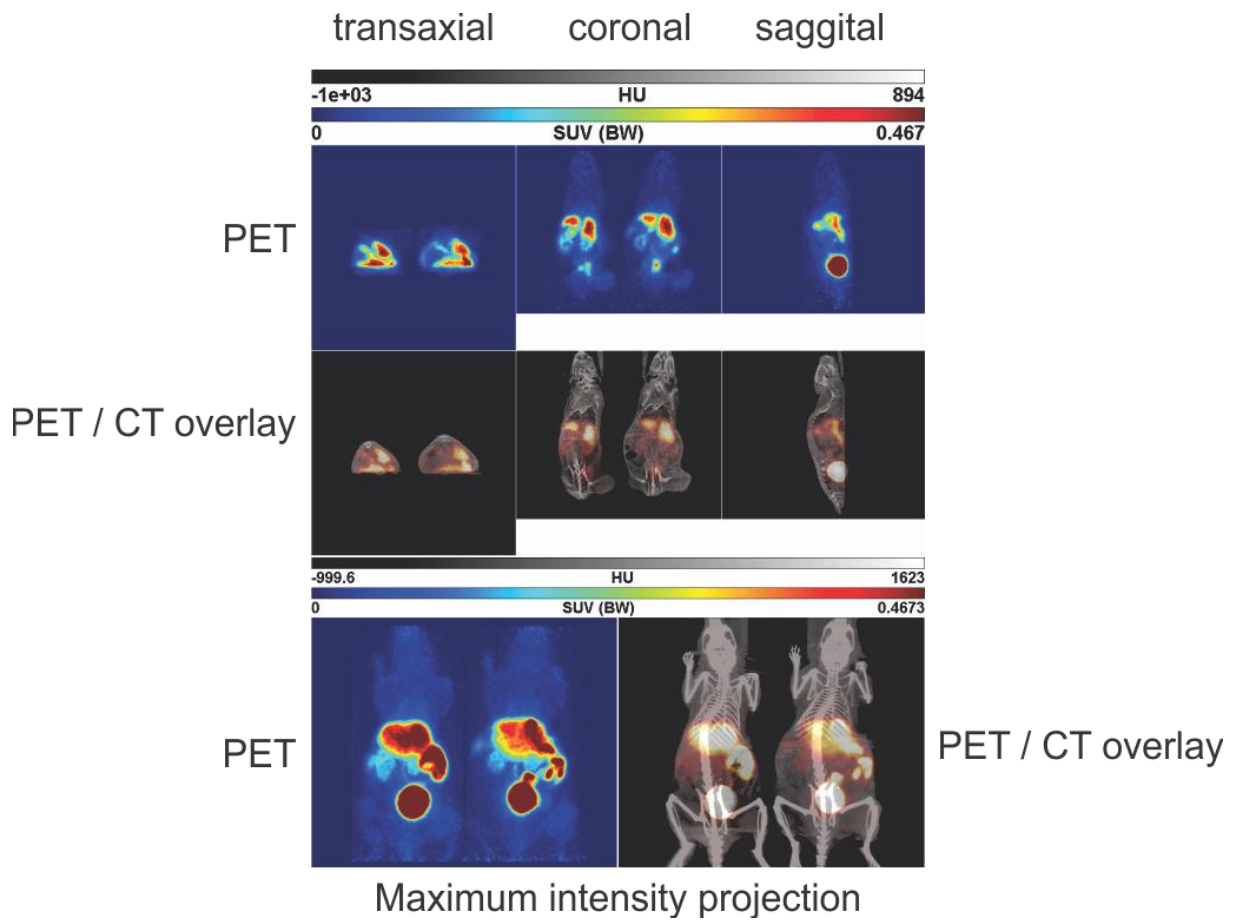


Figure S9 Orthogonal sections and maximum intensity projections of PET studies as separate PET and combined PET/CT images of [^{64}Cu]Cu-NOTA-CQDs at 60 min p.i. in two A431 tumor-bearing mice after single intravenous injection.

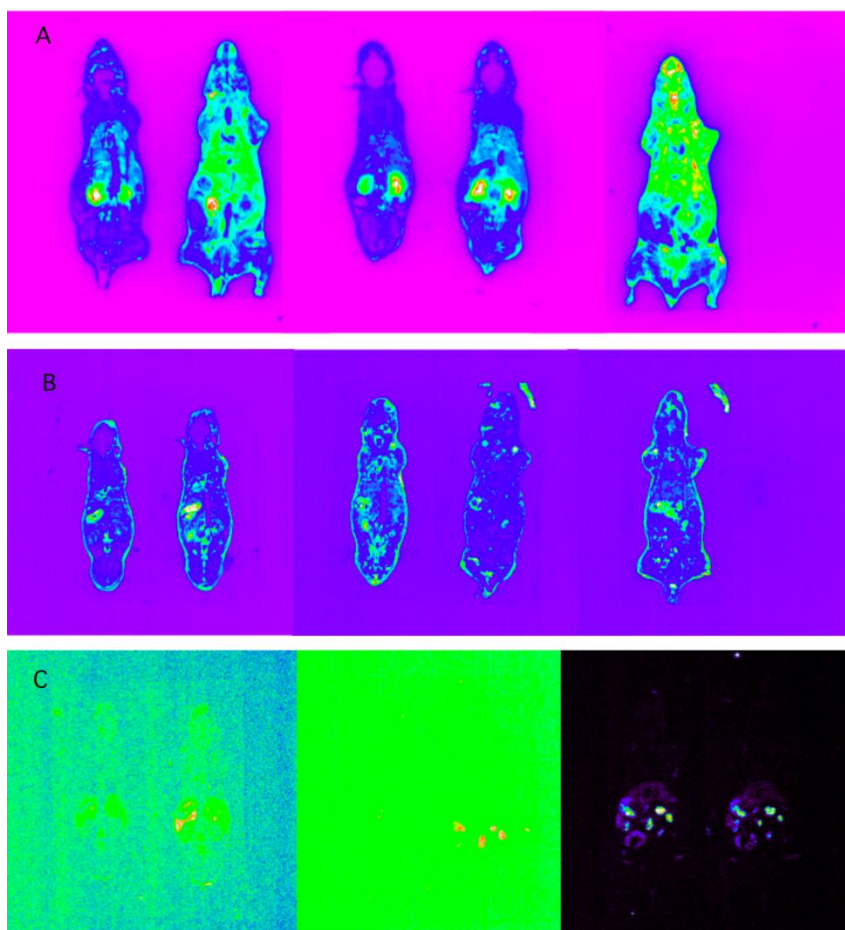


Figure S10 *Ex vivo* fluorescence images of whole body freeze sections (80 μm) of NMRI nu/nu mice at 5 min (A), 60 min (B) and 24 h (C) after single intravenous injection of Kodak-XS-670-labeled Si NPs-micro.

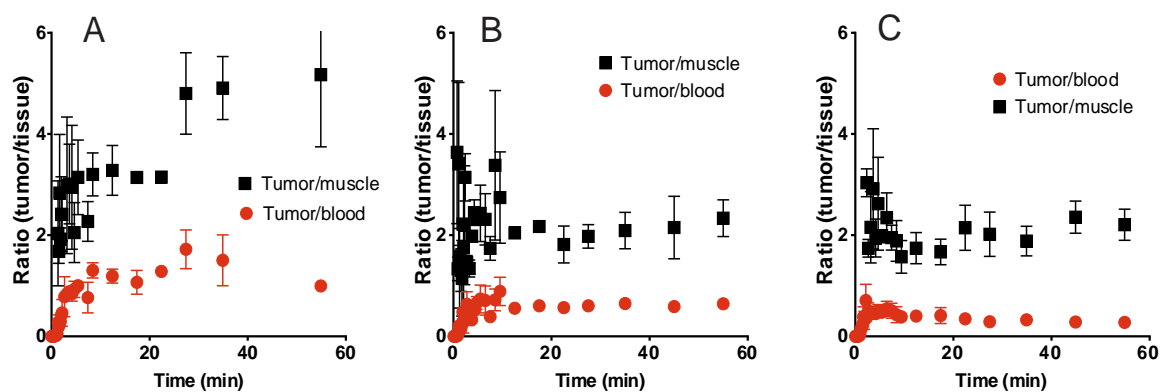


Figure S11 Tumor to tissue time curves derived from kinetic PET studies of $[^{64}\text{Cu}]\text{Cu-NOTA-Si NPs-hydro}$ (A), $[^{64}\text{Cu}]\text{Cu-NOTA-Si NPs-micro}$ (B) and $[^{64}\text{Cu}]\text{Cu-NOTA-CQDs}$ (C) in A431 tumor-bearing mice after single intravenous injection.

Table S1 Amount of [⁶⁴Cu]Cu-NOTA-Si NPs-hydro, [⁶⁴Cu]Cu-NOTA-Si NPs-micro, and [⁶⁴Cu]Cu-NOTA-CQDs in selected organs, and excretion in rats at 5 and 60 min after single intravenous application. Data expressed as % ID (mean ± SEM, n=4).

%ID	[⁶⁴ Cu]Cu-NOTA Si NP-hydro	[⁶⁴ Cu]Cu-NOTA Si NP-hydro	[⁶⁴ Cu]Cu-NOTA Si NP-micro	[⁶⁴ Cu]Cu-NOTA Si NP-micro	[⁶⁴ Cu]Cu-NOTA CQDs	[⁶⁴ Cu]Cu-NOTA CQDs
Time p.i. (min)	5	60	5	60	5	60
Brain	0.06 ± 0.00	0.02 ± 0.01	0.05 ± 0.01	0.02 ± 0.00	0.07 ± 0.01	0.02 ± 0.00
Pancreas	0.11 ± 0.01	0.07 ± 0.09	0.08 ± 0.01	0.03 ± 0.00	0.08 ± 0.02	0.05 ± 0.01
Spleen	0.09 ± 0.00	0.04 ± 0.04	0.08 ± 0.01	0.03 ± 0.00	0.36 ± 0.09	0.26 ± 0.05
Adrenals	0.04 ± 0.01	0.00 ± 0.00	0.02 ± 0.00	0.00 ± 0.00	0.04 ± 0.00	0.01 ± 0.00
Kidneys	11.5 ± 3.85	1.66 ± 0.03	10.2 ± 1.65	3.89 ± 0.25	7.65 ± 3.33	2.84 ± 0.22
Heart	0.25 ± 0.01	0.04 ± 0.03	0.17 ± 0.02	0.06 ± 0.00	0.32 ± 0.07	0.06 ± 0.00
Lung	0.75 ± 0.06	0.08 ± 0.00	0.56 ± 0.07	0.22 ± 0.01	1.18 ± 0.09	0.48 ± 0.03
Thymus	0.28 ± 0.07	0.02 ± 0.00	0.12 ± 0.03	0.05 ± 0.00	0.22 ± 0.06	0.06 ± 0.01
Thyroid	0.10 ± 0.00	0.01 ± 0.00	0.04 ± 0.00	0.03 ± 0.01	0.07 ± 0.02	0.04 ± 0.00
Hard.gl.	0.06 ± 0.03	0.03 ± 0.02	0.07 ± 0.01	0.01 ± 0.00	0.08 ± 0.02	0.04 ± 0.03
Liver	4.42 ± 0.88	1.41 ± 0.07	9.79 ± 1.59	2.66 ± 0.18	13.1 ± 0.48	14.9 ± 0.41
Femur	0.40 ± 0.06	0.06 ± 0.03	0.24 ± 0.06	0.07 ± 0.00	0.43 ± 0.06	0.21 ± 0.01
Testes	0.75 ± 0.12	0.19 ± 0.15	0.46 ± 0.08	0.15 ± 0.01	0.51 ± 0.14	0.18 ± 0.02
Intestine	3.15 ± 0.37	8.58 ± 3.64	15.7 ± 1.21	25.3 ± 2.46	5.14 ± 0.18	7.57 ± 3.72
Stomach	0.90 ± 0.09	2.93 ± 4.01	0.80 ± 0.42	3.25 ± 2.57	0.85 ± 0.14	2.16 ± 2.29
Urine calc.	10.7 ± 4.41	69.9 ± 6.13	19.2 ± 4.83	46.7 ± 4.53	5.38 ± 9.16	52.8 ± 5.06
%ID	[⁶⁴ Cu]Cu-NOTA NP- hydro	[⁶⁴ Cu]Cu-NOTA NP- hydro	[⁶⁴ Cu]Cu-NOTA NP- micro	[⁶⁴ Cu]Cu-NOTA NP- micro	[⁶⁴ Cu]Cu-NOTA CQDs	[⁶⁴ Cu]Cu-NOTA CQDs
Time p.i. (min)	5	60	5	60	5	60
renal	22.2 ± 8.26	71.6 ± 6.17	29.5 ± 6.49	50.6 ± 4.78	13.0 ± 12.5	55.7 ± 5.29
hepatobili ary	7.57 ± 1.25	9.99 ± 3.72	25.5 ± 2.81	27.9 ± 2.65	18.2 ± 0.67	22.5 ± 4.13

Table S2 Concentration of [⁶⁴Cu]Cu-NOTA-Si NPs-hydro, [⁶⁴Cu]Cu-NOTA-Si NPs-micro and [⁶⁴Cu]Cu-NOTA-CQDs in selected organs, tissues, and excretion in rats at 5 and 60 min after single intravenous application. Data expressed as SUV (mean ± SEM, n=4).

SUV (g/g)	[⁶⁴ Cu]Cu-NOTA Si NP-hydro	[⁶⁴ Cu]Cu-NOTA Si NP-hydro	[⁶⁴ Cu]Cu-NOTA Si NP-micro	[⁶⁴ Cu]Cu-NOTA Si NP-micro	[⁶⁴ Cu]Cu-NOTA CQDs	[⁶⁴ Cu]Cu-NOTA CQDs
Time p.i. (min)	5	60	5	60	5	60
Blood	1.44 ± 0.17	0.09 ± 0.00	1.22 ± 0.03	0.41 ± 0.03	1.00 ± 0.14	0.20 ± 0.02
BAT	0.81 ± 0.06	0.20 ± 0.14	0.40 ± 0.02	0.13 ± 0.01	0.63 ± 0.05	0.14 ± 0.01
Skin	1.46 ± 0.08	0.17 ± 0.04	0.83 ± 0.04	0.33 ± 0.04	1.07 ± 0.05	0.28 ± 0.05
Brain	0.04 ± 0.00	0.01 ± 0.00	0.05 ± 0.00	0.02 ± 0.00	0.04 ± 0.00	0.01 ± 0.00
Pancreas	0.46 ± 0.04	0.36 ± 0.47	0.43 ± 0.07	0.15 ± 0.01	0.41 ± 0.06	0.18 ± 0.04
Spleen	0.40 ± 0.04	0.21 ± 0.23	0.32 ± 0.05	0.14 ± 0.02	1.67 ± 0.46	1.17 ± 0.21
Adrenals	1.02 ± 0.09	0.16 ± 0.09	0.56 ± 0.10	0.16 ± 0.03	1.06 ± 0.04	0.46 ± 0.05
Kidneys	11.1 ± 3.40	1.71 ± 0.07	10.5 ± 0.88	4.27 ± 0.49	7.85 ± 2.98	2.69 ± 0.24
WAT	1.80 ± 1.62	0.27 ± 0.16	0.51 ± 0.22	0.08 ± 0.02	3.67 ± 5.16	0.27 ± 0.23
Muscle	0.43 ± 0.06	0.04 ± 0.00	0.31 ± 0.05	0.08 ± 0.01	0.35 ± 0.03	0.07 ± 0.00
Heart	0.59 ± 0.01	0.09 ± 0.06	0.45 ± 0.02	0.16 ± 0.01	0.67 ± 0.09	0.14 ± 0.00
Lung	1.04 ± 0.04	0.12 ± 0.00	0.81 ± 0.08	0.33 ± 0.02	1.69 ± 0.14	0.63 ± 0.04
Thymus	3.27 ± 4.74	0.07 ± 0.01	0.34 ± 0.03	0.14 ± 0.01	0.52 ± 0.09	0.17 ± 0.02
Hard.gl.	0.28 ± 0.23	0.18 ± 0.12	0.52 ± 0.08	0.16 ± 0.02	0.57 ± 0.23	0.29 ± 0.29
Liver	0.95 ± 0.10	0.33 ± 0.04	1.85 ± 0.14	0.52 ± 0.06	2.29 ± 0.06	2.58 ± 0.23
Femur	0.71 ± 0.06	0.11 ± 0.05	0.52 ± 0.09	0.16 ± 0.00	0.78 ± 0.05	0.34 ± 0.02
Testes	0.55 ± 0.09	0.12 ± 0.09	0.38 ± 0.07	0.11 ± 0.01	0.44 ± 0.14	0.15 ± 0.02

Table S3 Best fit values according the one-phase decay model of the [⁶⁴Cu]Cu-NOTA-Si NPs-hydro, [⁶⁴Cu]Cu-NOTA-Si NPs-micro and [⁶⁴Cu]Cu-NOTA-CQDs clearance from the blood (mean values of 4 animals).

	[⁶⁴ Cu]Cu-NOTA Si NP-hydro	[⁶⁴ Cu]Cu-NOTA Si NP-micro	[⁶⁴ Cu]Cu-NOTA CQDs
One phase decay			
Best-fit values			
Y0	2,131	1,917	2,641
Plateau	0,1598	0,2969	1,121
K	0,08450	0,06583	0,06101
Half Life	8,203	10,53	11,36
Tau	11,83	15,19	16,39
Span	1,971	1,621	1,520
Goodness of Fit			
Degrees of Freedom	21	21	69
R square (weighted)	0,8252	0,9095	0,4187
Weighted Sum of Squares (1/Y ²)	1,839	0,5186	5,570
Sy.x	0,2959	0,1571	0,2841
Normality of Residuals			
D'Agostino & Pearson omnibus K2	0,4478	3,118	0,01599
P value	0,7994	0,2104	0,9920
Passed normality test (alpha=0.05)?	Yes	Yes	Yes
P value summary	ns	ns	ns
Constraints			
K	K > 0,0	K > 0,0	K > 0,0
Number of points			
Analyzed	24	24	72
Outliers (excluded, Q=1.0%)	0	0	0

Table S4 Best fit values according the one-phase association model of the [⁶⁴Cu]Cu-NOTA-Si NPs-hydro, [⁶⁴Cu]Cu-NOTA-Si NPs-micro, and [⁶⁴Cu]Cu-NOTA-CQDs accumulation in the urine (mean values of 4 animals).

	[⁶⁴ Cu]Cu-NOTA Si NP-hydro	[⁶⁴ Cu]Cu-NOTA Si NP-micro	[⁶⁴ Cu]Cu-NOTA CQDs
One-phase association			
Best-fit values			
Y0	-18,08	1,034	-3,183
Plateau	84,51	67,39	55,89
K	0,07468	0,08022	0,07010
Tau	13,39	12,47	14,27
Half-time	9,282	8,640	9,888
Span	102,6	66,36	59,07
Goodness of Fit			
Degrees of Freedom	21	21	65
R square (weighted)	0,9888	0,8191	0,8735
Weighted Sum of Squares (1/Y ²)	0,06944	0,5951	1,640
Sy.x	0,05750	0,1683	0,1588
Normality of Residuals			
D'Agostino & Pearson omnibus K2	5,789	1,270	0,7400
P value	0,0553	0,5299	0,6907
Passed normality test (alpha=0.05)?	Yes	Yes	Yes
P value summary	ns	ns	ns
Constraints			
K	K > 0,0	K > 0,0	K > 0,0
Number of points			
Analyzed	24	24	68
Outliers (excluded, Q=1.0%)	0	0	1